lenses, i.e., n positive lenses and n negative lenses. There are therefore $2n$ lenses, all of which have random lateral displacements with an rms value of σ.

For the case of positive lenses spaced confocally and equal power negative lenses ($\alpha=\beta=1$), then

$$\sqrt{\langle r_{n+1}^2\rangle} = 2.82\sigma\sqrt{n}.$$

In the case of no negative lenses ($\alpha=0$, $\beta=1$), then

$$\sqrt{\langle r_{n+1}^2\rangle} = 1.41\sigma\sqrt{n}.$$

In the first case the expected deviation of the output beam is twice that of the second case, but there are twice as many lenses to align in the first case. If this increase in lateral sensitivity were due only to the increased number of lenses, one would expect an increase of only $\sqrt{2}$. The additional factor of $\sqrt{2}$ is due to the reduced focusing properties of the line.

Summary

As expected, the addition of the negative lenses reduces the ability of the transmission line to control the light beam. However, if the power of the negative lenses is kept equal to or less than the power of the positive lenses, the reduction in guiding ability is not too severe.

For example, consider a transmission line of positive lenses spaced confocally ($\beta=1$) and add negative lenses of the same power ($\alpha=1$):

1) The spot size at the positive lens is increased by 1.315.
2) The allowed bending radius is increased by 2.5.
3) The critical bending period is increased by 1.5.
4) The sensitivity to random lateral lens displacements is increased by 2.

References

[1] D. Marcuse and S. E. Miller, "Analysis of a tubular gas lens," *Bell Sys. Tech. J.*, vol. 43, pp. 1759–1782, July 1964.
[2] D. Marcuse, "Theory of a thermal gradient gas lens," *IEEE Transactions on Microwave Theory and Techniques*, vol. MTT-13, pp. 734–739, November 1965.
[3] W. H. Steier, "Measurements on a thermal gradient gas lens," *IEEE Transactions on Microwave Theory and Techniques*, vol. MTT-13, pp. 740–748, November 1965.
[4] A. C. Beck, "Thermal gas lens measurements," *Bell Sys. Tech. J.*, vol. 43, pp. 1818–1820, July 1964.
[5] D. Marcuse, "Properties of periodic gas lenses," *Bell Sys. Tech. J.*, vol. 44, pp. 2083–2116, November 1965.
[6] S. E. Miller, "Alternating-gradient focusing and related properties of convergent lens focusing," *Bell Sys. Tech. J.*, vol. 43, pp. 1741–1758, July 1964.
[7] H. Kogelnik, "Imaging of optical modes—Resonators with internal lenses," *Bell Sys. Tech. J.*, vol. 44, pp. 455–494, March 1965.
[8] W. W. Rigrod, "The optical ring resonator," *Bell Sys. Tech. J.*, vol. 44, pp. 907–916, May–June 1965.
[9] G. D. Boyd and J. P. Gordon, "Confocal multimode resonator for millimeter through optical wavelength masers," *Bell Sys. Tech. J.*, vol. 40, pp. 489–508, March 1961.
[10] S. E. Miller, "Directional control in light-wave guidance," *Bell Sys. Tech. J.*, vol. 43, pp. 1727–1741, July 1964.
[11] H. E. Rowe, private communication, November, 1964.
[12] P. K. Tien, J. P. Gordon, and J. R. Whinnery, "Focusing of a light beam of Gaussian field distribution in continuous and periodic lens-like media," *Proc. IEEE*, vol. 53, pp. 129–136, February 1965.
[13] J. Hirano and Y. Fukatsu, "Stability of a light beam in a beam waveguide," *Proc. IEEE*, vol. 52, pp. 1284–1292, November 1964.
[14] J. R. Pierce, *Theory and Design of Electron Beams*, 2nd ed. Princeton, N. J.: Van Nostrand, 1954.
[15] D. Marcuse, "Propagation of light rays through a lens-waveguide with curved axis," *Bell Sys. Tech. J.*, vol. 43, pp. 741–754, March 1964.
[16] H. G. Unger, "Light beam propagation in curved schlieren guides," *Arch. Elekt. Ubertragung*, vol. 19, pp. 189–198, April 1965.
[17] D. Marcuse, "Statistical treatment of light-ray propagation in beam-waveguides," *Bell Sys. Tech. J.*, vol. 44, pp. 2065–2082, November 1965.
[18] D. W. Berreman, "Growth of oscillations of a ray about the irregularly wavy axis of a lens light guide," *Bell Sys. Tech. J.*, vol. 44, pp. 2117–2132, November 1965.
[19] H. E. Rowe, private communication, June, 1963.

Mode Conversion in Tapered Waveguides At and Near Cutoff

C. C. H. TANG

Abstract—The coupling coefficient between the TE_{11} mode and the TM_{11} mode in tapered circular waveguides is derived, and at cutoff frequency it tends to approach an infinity of the order of $0^{-1/4}$. It is surprising to discover that the corresponding coupling coefficient between the TE_{10} mode and the TM_{12} mode in tapered rectangular waveguides approaches instead a zero of the order of $0^{1/4}$ at cutoff frequency. Accordingly, for the modes concerned, the choice of using circular or square waveguides as tapers for transition at and near cutoff frequency is significant in reducing mode conversion level. At and near cutoff frequency a "synthesized" square taper is better in that it is shorter than a "synthesized" circular taper for the same mode conversion levels. On the other hand, for frequencies far away from cutoff the choice is insignificant.

Design procedures for "synthesized" waveguide tapers at and near cutoff are presented, and the results of measurements are in agreement with the theoretical calculations.

Manuscript received December 14, 1965; revised February 10, 1966.

The author is with Bell Telephone Laboratories, Inc., Murray Hill, N. J.

Introduction

MODE CONVERSION in a tapered waveguide capable of multimode propagation had been analyzed [1]–[3] previously, but these analyses treated only the cases where the converted modes are also far away from cutoff, as the converting or exciting mode is. The present paper treats the case where the converted mode is at and near cutoff. The basic approach of the problem is the same as that shown in Tang [3], but the coupling coefficient between the converting mode and the converted mode has to be in a general form appropriate for all cases including at, near, and far away from cutoff.

Instead of treating the general problem of mode conversion at and near cutoff in tapered multimode waveguides, we shall study a specific example for purposes of illustration. The waveguide taper changing from a radius a_1 to radius a_2 in length l is shown in Fig. 1.

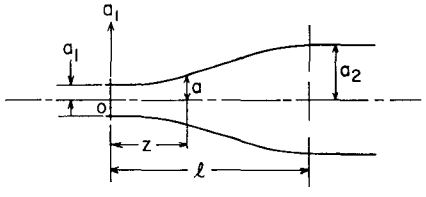

Fig. 1. A circular waveguide taper.

Assuming first that the dominant TE_{11} mode alone is excited in a multimode circular waveguide of radius a_1, we want to know what and how strong are the converted modes in the waveguide of radius a_2, provided the tapering is gentle. Calculation shows that the first few modes possible for propagation in a multimode waveguide taper appear in the following order for increasing radius: TE_{11}, TM_{01}, TE_{21}, TM_{11} and TE_{01}, TE_{31}, TM_{21}, TE_{41}, TE_{12}, TM_{02}, TM_{31}, TE_{51}, TE_{22}, TM_{12} and TE_{02}, etc. If the excitation is TE_{11} mode alone and the taper is axially straight and circularly symmetric, we can show by means of the orthogonality relation that the only converted modes will be of the TM_{1n} or (and) TE_{1n} type, depending on the actual size of the waveguide taper used. These converted modes will be present in the following order as the taper radius a increases: TM_{11}, TE_{12}, TM_{12}, TE_{13}, TM_{13}, etc. For simplicity we shall assume that the waveguide size is such that the only possible converted mode is the TM_{11} mode. In the next section the coupling coefficient between the TE_{11} mode and the TM_{11} mode of circular waveguides will be briefly derived; in addition, the corresponding coupling coefficient between the TE_{10} mode and the TM_{12} mode of rectangular waveguides will be derived also. It will be shown that at and near cutoff frequency the choice of using circular or rectangular waveguides as tapers is significant in reducing mode conversion level.

Formulation

The coupling coefficient between the TE_{11} mode and the TM_{11} mode in circular waveguide can be obtained by converting Maxwell's equations with appropriate boundary conditions into generalized telegraphist's equations as shown by Schelkunoff [4]. The field configuration of the TE_{11} and TM_{11} modes at any cross section in circular waveguides can be represented by

$$
\begin{aligned}
E_\rho &= \frac{B}{p\rho} V(z) J_1(p\rho) \sin\theta + \overline{BV}(z) J_1'(q\rho) \sin\theta \\
E_\theta &= BV(z) J_1'(p\rho) \cos\theta + \frac{\overline{B}}{q\rho} \overline{V}(z) J_1(q\rho) \cos\theta \\
E_z &= j \frac{\overline{B}q}{\omega\epsilon} \overline{I}(z) J_1(q\rho) \sin\theta \\
H_\rho &= -BI(z) J_1'(p\rho) \cos\theta - \frac{\overline{B}}{q\rho} \overline{I}(z) J_1(q\rho) \cos\theta \\
H_\theta &= \frac{B}{p\rho} I(z) J_1(p\rho) \sin\theta + \overline{BI}(z) J_1'(q\rho) \sin\theta \\
H_z &= -j \frac{B\rho}{\omega\mu} V(z) J_1(p\rho) \cos\theta
\end{aligned} \tag{1}
$$

where

$$
\begin{aligned}
B^{-2} &= \int_0^a \left\{ [J_1^2(p\rho)]^2 + \left[\frac{J_1(p\rho)}{p\rho} \right]^2 \right\} \rho \, d\rho \\
&= \int_0^a J_1^2(p\rho) \rho \, d\rho, \\
\overline{B}^{-2} &= \int_0^a \left\{ [J_1^2(q\rho)]^2 + \left[\frac{J_1(q\rho)}{q\rho} \right]^2 \right\} \rho \, d\rho \\
&= \int_0^a J_1^2(q\rho) \rho \, d\rho,
\end{aligned} \tag{2}
$$

and

$$
p(z) = \frac{k_{11}}{a(z)} \quad (k_{11} \text{ is the first root of } J_1'),
$$

$$
q(z) = \frac{\bar{k}_{11}}{a(z)} \quad (\bar{k}_{11} \text{ is the first root } J_1).
$$

Prime (′) denotes the derivative with respect to its argument, and barred letters denote quantities related to TM mode. The boundary condition along the tapered section is, at $\rho = a$,

$$
E_z(a, z) = -E_\rho(a, z) \frac{da}{dz}. \tag{3}
$$

Substituting (1) into Maxwell's equations in cylindrical coordinates with due care exercised on differentiation processes because of the boundary condition along the tapered section, and performing the integration from $\rho = 0$ to $\rho = a$ and from $\theta = 0$ to $\theta = 2\pi$ on these equations

with appropriate normalizing factors and weighting functions, we obtain the following differential equations in telegraphist's form:

$$\begin{aligned}
\frac{dI}{dz} &= -\frac{\gamma^2}{j\omega\mu}V + \frac{1}{k_{11}^2-1}\frac{1}{a}\frac{da}{dz}I + \frac{2}{(k_{11}^2-1)^{1/2}}\frac{1}{a}\frac{da}{dz}\bar{I} \\
\frac{dV}{dz} &= -j\omega\mu I - \frac{1}{k_{11}^2-1}\frac{1}{a}\frac{da}{dz}V \\
\frac{d\bar{I}}{dz} &= -j\omega\epsilon\bar{V} + \frac{1}{a}\frac{da}{dz}\bar{I} \\
\frac{d\bar{V}}{dz} &= -\frac{\bar{\gamma}^2}{j\omega\epsilon}\bar{I} - \frac{1}{a}\frac{da}{dz}\bar{V} - \frac{2}{(k_{11}^2-1)^{1/2}}\frac{1}{a}\frac{da}{dz}V
\end{aligned} \tag{4}$$

$$\begin{aligned}
\frac{dA}{dz} &= -\gamma(z)A + \zeta(z)\bar{A} \\
\frac{d\bar{A}}{dz} &= -\bar{\gamma}(z)\bar{A} - \zeta(z)A
\end{aligned} \tag{8}$$

where

$$\zeta(z) = \left[\frac{Z}{\bar{Z}}\frac{1}{(k_{11}^2-1)}\right]^{1/2}\frac{1}{a}\frac{da}{dz} \tag{9}$$

is the coupling coefficient between the TE_{11} and TM_{11} forward waves. Substituting (7) into (9), we obtain the general coupling coefficient in the following explicit form:

$$\begin{aligned}
\zeta(z) &= \left[\frac{1}{(k_{11}^2-1)\left(1-\frac{p^2}{\omega^2\epsilon\mu}\right)^{1/2}\left(1-\frac{q^2}{\omega^2\epsilon\mu}\right)^{1/2}}\right]^{1/2}\frac{1}{a}\frac{da}{dz} \\
&= \frac{1}{(k_{11}^2-1)^{1/2}}\cdot\frac{1}{\left[\left(a^2-\frac{k_{11}^2\lambda_0^2}{4\pi^2}\right)\left(a^2-\frac{\bar{k}_{11}^2\lambda_0^2}{4\pi^2}\right)\right]^{1/4}}\cdot\frac{da}{dz}
\end{aligned} \tag{10}$$

where

$$\gamma^2(z) = p^2(z) - \omega^2\epsilon\mu, \text{ and } \bar{\gamma}^2(z) = q^2(z) - \omega^2\epsilon\mu. \tag{5}$$

For the lossless case,

$$\gamma = j\beta, \quad \text{and} \quad \bar{\gamma} = j\bar{\beta}. \tag{5'}$$

From (4) we notice that the coupling of the TM_{11} mode due to the presence of the TE_{11} mode is of the voltage type only, whereas the coupling of the TE_{11} mode due to the presence of the TM_{11} mode is of the current type only.

If we let A and R represent the amplitudes of the forward and reflected waves, respectively, the following equations are always true:

$$\begin{aligned}
V &= \sqrt{Z}(A+R), \qquad \bar{V} = \sqrt{\bar{Z}}(\bar{A}+\bar{R}) \\
I &= \frac{1}{\sqrt{Z}}(A-R), \qquad \bar{I} = \frac{1}{\sqrt{\bar{Z}}}(\bar{A}-\bar{R})
\end{aligned} \tag{6}$$

where

$$Z(z) = \frac{j\omega\mu}{\gamma(z)}, \quad \text{and} \quad \bar{Z}(z) = \frac{\bar{\gamma}(z)}{j\omega\epsilon}. \tag{7}$$

Substitution of (6) into (4) results in a new set of four coupled differential equations in forward waves and reflected waves. If the taper is gentle, we can assume reflections and multiple reflections to be negligibly small, and obtain the following pair of coupled differential equations in forward-wave amplitudes:

where λ_0 is the free-space wavelength. For frequencies far away from cutoff, (10) reduces to the simple form

$$\zeta(z) = \frac{1}{(k_{11}^2-1)^{1/2}}\cdot\frac{1}{a}\frac{da}{dz}. \tag{11}$$

For frequencies at cutoff we notice from (10) that there is an apparent zero in the denominator, and the coupling coefficient appears to be infinite. On the other hand, (10) is obviously integrable in the cutoff region along the taper since the zero in the denominator is of the order of $0^{1/4}$.

From the point of view of reducing reflections and mode conversions, tapers should be designed with profiles having zero derivatives at the ends. The stipulation of zero slope at the ends of the taper also makes it possible to utilize the results presented in Tang [3], namely, (29), which is the solution of (8) here, and Fig. 2 in that reference. A choice of appropriate n and ρ_1 from Fig. 2 of Tang [3] for a prescribed mode conversion level, together with the following pair of parametric equations, should give us the proper profile of the desired "optimum" taper:

$$\int_0^z \zeta\, dz \doteq \int_0^\rho (2\theta)\, d\rho, \tag{12}$$

i.e.,

$$\frac{1}{(k_{11}^2-1)^{1/2}}\int_{a1}^{a}\frac{da}{\left[\left(a^2-\frac{k_{11}^2\lambda_0^2}{4\pi^2}\right)\left(a^2-\frac{k_{11}^2\lambda_0^2}{4\pi^2}\right)\right]^{1/4}} = \int_0^\rho C_n \sin^n\left(\frac{\pi\rho}{\rho_1}\right)d\rho, \tag{12'}$$

and

$$z = \int_0^{\rho} \frac{d\rho}{\Gamma} \doteq \int_0^{\rho} \frac{d\rho}{\Delta\beta} = \int_0^{\rho} \frac{d\rho}{\frac{1}{2}(\beta - \bar{\beta})}, \tag{13}$$

i.e.,

$$z = \frac{\lambda_0}{\pi} \int_0^{\rho} \frac{a\, d\rho}{\left[\left(a^2 - \frac{k_{11}^2\lambda_0^2}{4\pi^2}\right)^{1/2} - \left(a^2 - \frac{\bar{k}_{11}^2\lambda_0^2}{4\pi^2}\right)^{1/2}\right]}, \tag{13'}$$

where C_n is a constant to be determined by the boundary conditions: at

$$a = a_1,\ \rho = 0, \quad \text{and} \quad a = a_2,\ \rho = \rho_1. \tag{14}$$

Equations (12′) and (13′) have to be integrated numerically.

We now turn to a brief derivation of the coupling coefficient between the TE_{10} mode and the TM_{12} mode of rectangular or square waveguides. These two modes are the counterparts of the TE_{11} and TM_{11} modes in circular waveguides, and therefore a detailed study of the coupling coefficient between these two modes in rectangular or square waveguide may throw some new light on the problem of mode conversion at cutoff. The field configuration of the TE_{10} and TM_{12} modes at any rectangular cross section, as shown in Fig. 2, can be represented by

$$\begin{aligned}
H_x &= -CI(z)\cos\frac{\pi x}{a} + \bar{C}\bar{I}(z)\cos\frac{\pi x}{a}\cos\frac{2\pi y}{b} \\
H_y &= \frac{b}{2a}\bar{C}\bar{I}(z)\sin\frac{\pi x}{a}\sin\frac{2\pi y}{b} \\
H_z &= C\frac{a}{\pi}\frac{k_{10}^2}{j\omega\mu}V(z)\sin\frac{\pi x}{a} \\
E_x &= \frac{b}{2a}\bar{C}\bar{V}(z)\sin\frac{\pi x}{a}\sin\frac{2\pi y}{b} \\
E_y &= CV(z)\cos\frac{\pi x}{a} - \bar{C}\bar{V}(z)\cos\frac{\pi x}{a}\cos\frac{2\pi y}{b} \\
E_z &= \frac{b}{2\pi}\bar{C}\frac{k_{12}^2}{j\omega\epsilon}\bar{I}(z)\cos\frac{\pi x}{a}\sin\frac{2\pi y}{b}
\end{aligned} \tag{15}$$

where

$$\begin{aligned}
C &= \frac{\pi}{a}\frac{1}{k_{10}}\frac{2}{\sqrt{ab}} \\
\bar{C} &= \frac{2\pi}{b}\frac{1}{\bar{k}_{12}}\frac{2}{\sqrt{ab}}
\end{aligned} \tag{16}$$

and

$$k_{mn}(z) = \sqrt{\left(\frac{m\pi}{a(z)}\right)^2 + \left(\frac{n\pi}{b(z)}\right)^2} = \bar{k}_{mn}(z). \tag{17}$$

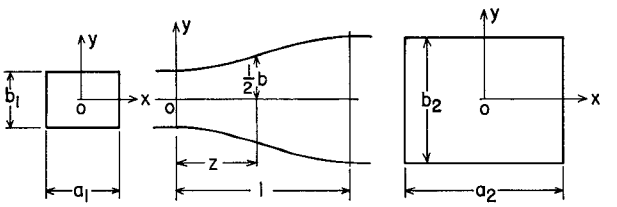

Fig. 2. A rectangular waveguide taper.

The boundary condition along the tapered section is

$$\begin{aligned}
E_z &= -\frac{1}{2}\left(E_x\frac{da}{dz}\right), \qquad x = \pm\frac{a}{2} \\
E_z &= -\frac{1}{2}\left(E_y\frac{db}{dz}\right), \qquad y = \pm\frac{b}{2}.
\end{aligned} \tag{18}$$

Substituting (15) into Maxwell's equations in rectangular coordinates with due care exercised on differentiation processes, and performing the integration over the cross section on these equations with appropriate normalizing factors, we obtain the following equations:

$$\begin{aligned}
\frac{dI}{dz} &= -\frac{\Gamma^2}{j\omega\mu}V + \left(\frac{1}{C}\frac{dC}{dz} - \frac{1}{2}\frac{1}{a}\frac{da}{dz}\right)I \\
\frac{dV}{dz} &= -j\omega\mu I - \left(\frac{1}{C}\frac{dC}{dz} - \frac{1}{2}\frac{1}{a}\frac{da}{dz}\right)V + \frac{\bar{C}}{C}\frac{1}{b}\frac{db}{dz}\bar{V} \\
\frac{d\bar{I}}{dz} &= -j\omega\epsilon\bar{V} - \frac{1}{4}ab\bar{C}^2\left(\frac{b^2}{4a^2}\frac{1}{a}\frac{da}{dz} + \frac{1}{b}\frac{db}{dz}\right)\bar{I} \\
&\quad - \frac{1}{2}aC\bar{C}\frac{db}{dz}I \\
\frac{d\bar{V}}{dz} &= -\frac{\bar{\Gamma}^2}{j\omega\epsilon}\bar{I} + \frac{1}{4}ab\bar{C}^2\left(\frac{b^2}{4a^2}\frac{1}{a}\frac{da}{dz} + \frac{1}{b}\frac{db}{dz}\right)\bar{V}
\end{aligned} \tag{19}$$

where

$$\Gamma^2(z) = k_{10}^2(z) - \omega^2\epsilon\mu, \text{ and } \bar{\Gamma}^2(z) = \bar{k}_{12}^2(z) - \omega^2\epsilon\mu. \tag{20}$$

Note that in (19)

$$\frac{\bar{C}}{C}\frac{1}{b}\frac{db}{dz} = \frac{1}{2}aC\bar{C}\frac{db}{dz} = \frac{2\sqrt{2}\pi}{\bar{k}_{12}}\frac{1}{b^2}\frac{db}{dz} \tag{21}$$

as expected. Inspection of (19) reveals that the nature of the coupling mechanism is just the reverse of that of the circular waveguide case; i.e., the coupling of the TM_{12} mode due to the presence of the TE_{10} mode is of the current type only, whereas the coupling of the TE_{10} mode due to the presence of the TM_{12} mode is of the voltage type only.

For gentle tapers reflections can be neglected and (19) can be converted into a pair of coupled equations in forward waves F and $\bar{F}$ as

$$\begin{aligned}
\frac{dF}{dz} &= -\Gamma(z)F + \zeta'(z)\bar{F} \\
\frac{d\bar{F}}{dz} &= -\bar{\Gamma}(z)\bar{F} - \zeta'(z)F
\end{aligned} \tag{22}$$

where

$$\zeta'(z) = \frac{\sqrt{2}\pi}{\bar{k}_{12}}\sqrt{\frac{\bar{K}}{K}}\,\frac{1}{b^2}\,\frac{db}{dz} \tag{23}$$

and

$$K(z) = \frac{j\omega\mu}{\Gamma(z)}, \quad \text{and} \quad \bar{K}(z) = \frac{\bar{\Gamma}(z)}{j\omega\epsilon}. \tag{24}$$

Note that ζ' is proportional to db/dz only, and independent of da/dz for coupling between the TE_{10} mode and the TM_{12} mode. Combining (23), (24), and (17), we obtain the coupling coefficient explicitly as

$$\zeta'(z) = \frac{\sqrt{2}a}{(4a^2+b^2)^{1/2}}\left\{\left[1-\left(\frac{\lambda_0}{2a}\right)^2\right]\cdot\left[1-\frac{(4a^2+b^2)\lambda_0^2}{(2ab)^2}\right]\right\}^{1/4}\frac{1}{b}\,\frac{db}{dz}. \tag{25}$$

For a square guide $a=b$, (25) reduces to

$$\zeta_{a=}'(z) = \frac{2}{\sqrt{10}}\left\{\left[b^2-\left(\frac{\lambda_0}{2}\right)^2\right]\cdot\left[b^2-\left(\frac{\sqrt{5}\lambda_0}{2}\right)^2\right]\right\}^{1/4}\frac{1}{b^2}\,\frac{db}{dz}. \tag{26}$$

For frequencies far away from cutoff, (25) and (26) reduce to, respectively,

$$\zeta'(z) = \frac{\sqrt{2}a}{(4a^2+b^2)^{1/2}b}\,\frac{db}{dz}, \tag{27}$$

and

$$\zeta_{a=}'(z) = \frac{2}{\sqrt{10}}\,\frac{1}{b}\,\frac{db}{dz}. \tag{28}$$

At cutoff it is clear from (25) or (26) that the coupling coefficient ζ' vanishes to a zero of the order of $0^{1/4}$ in contrast to the circular waveguide case where the coupling coefficient ζ of (10) at cutoff becomes infinite of the order of $0^{-1/4}$.

From a purely theoretical point of view, we can conclude now that in order to reduce the mode conversion levels in tapers near and at cutoff frequency region, it is more desirable to use for the modes concerned rectangular or square waveguides than circular waveguides. On the other hand, when the tapers are for frequencies far away from cutoff, the choice between the circular waveguide and the rectangular waveguide becomes insignificant as evidenced by the fact that the magnitude of ζ' of (28) is about the same as that of ζ of (11).

Designs and Experiments

The following theoretical requirements and experimental setup are given: A pure TE_{10} mode is successfully excited in a square (1.79 in) waveguide, and the receiving end waveguide is required to be circular (2.812 in ID). Design a transition section such that the conversion of the TM_{11} mode is at least 43 dB less than the TE_{11} mode in the circular waveguide within the frequency range from 5725 Mc/s to 6425 Mc/s.

The required transition section is square (1.79 in) at one end and circular (2.812 in ID) at the other end. Depending upon the choice of design scheme, the major part of the transition section can be in either circular waveguide taper or square waveguide taper. We shall design first a circular taper and then a square taper for purposes of comparison.

Circular Tapers

Calculation shows that the TM_{11} mode at $f=6425$ Mc/s and $f=5925$ Mc/s does not propagate until the diameter of the circular waveguide is 2.242 in and 2.432 in, respectively. Accordingly, the circular taper should be designed at $f=6425$ Mc/s with $2a_1=2.242$ in and $2a_2=2.812$ in. To complete the transition section from 1.79 in square to 2.812 in ID circular, we need another section with 1.79 in square at one end to 2.242 in ID circular at the other end in addition to the $2a_1=2.242$ in to $2a_2=2.812$ in circular taper. Since the TM_{11} mode at $f=6425$ Mc/s cannot propagate in the section from 1.79 in square to 2.242 in ID circular, the design of such a section does not involve the TM_{11} mode conversion but does affect the reflection level of the dominant mode. To simplify the fabrication processes, this section can be made from a mandrel formed simply by cutting a linear conical taper with $2a_1=2.242$ in and $2a_2=\sqrt{2}\times 1.79$ in and slicing off four flat sides with the slope (2.242–1.79 in)$2l$ such that one end is a circle of 2.242 in diameter and the other end is a square of 1.79 in side. The dominant mode reflection from this section of length $l=12$ in is about -45 dB by measurements.

The exact profile of the circular taper from $2a_1=2.242$ in to $2a_2=2.812$ in is obtained by solving the pair of parametric equations (12′) and (13′). The choice of appropriate n and ρ_1 from Fig. 2 of Tang [3] deserves some detailed discussion. From Tang [3] we understand that the parameter ρ_1 for a gentle taper is approximately the integral (over the length of the taper) of one half the difference of the phase constants of the two modes involved in conversion. For frequencies far away from cutoff, ρ_1 increases for decreasing frequencies, and accordingly a taper is always designed for the highest frequency in the band so that its performance at lower frequencies is always better than the prescribed. For frequencies at and near cutoff, however, ρ_1 decreases for decreasing frequencies, and therefore mode conversion increases with decreasing frequencies. Our present prescription also requires that the taper be designed for the highest frequency in the band, and consequently we have to know approximately the value of ρ_1 for the lowest frequency in the band. On the other hand, we cannot obtain the value of ρ_1 for the lowest frequency until the required profile is provided. Clearly, we have to employ some "cut-and-try" processes in choosing the values of n and ρ_1 for the highest frequency at a mode

conversion level much less than the prescribed level. With the chosen values of n and ρ_1 we can obtain the profile and therefore the approximate value of ρ_1 for the lowest frequency. If this value of ρ_1 for the lowest frequency meets the prescribed requirements, we have succeeded in designing the taper. If not, we have to try another set of values for n and ρ_1 for the highest frequency. By choosing $n=3$ and $\rho_1=15.5$ for the highest frequency at about -58 dB mode conversion, we succeed in obtaining a taper having about -43 dB mode conversion at the lowest frequency. The length of the taper by this "synthesis" method turns out to be about 20 in, and the profile is monotonically increasing in a "sophisticated" manner.

For purposes of experimental comparison, another circular taper from $2a_1=2.242$ in to $2a_2=2.812$ in is fabricated with the following "simple" profile:

$$a = a_1 + (a_2 - a_1)\sin^2\left(\frac{\pi}{2}\frac{z}{l}\right) \tag{29}$$

where l is arbitrarily taken to be 23 in. Note this profile also has zero initial derivative only at the design frequency (i.e., the highest frequency in the band).

The results of the measurements by Klinger's method [5] are tabulated in Table I. Obviously, the 23-in taper of "simple" profile does not meet the requirement by about 14 dB in the high-frequency region. The fact that the measured mode conversion levels of the "synthesized" circular taper are flat over the band is mainly due to the accuracy limit of the measuring equipment.

TABLE I

TM_{11} Mode Conversion Level in dB

Frequency (Mc/s)	20 in Circular Taper by "Synthesis" Method	23 in Circular Taper $\Delta a\alpha \sin^2(\pi/2\, z/l)$	11 in "Linear" Square Taper
5925	−43	−43	−43
6000	−43	−43	−42
6100	−43	−43	−43
6200	−43	−43	−43
6300	−43	−41	−43
6400	−43	−33	−41
6425	−43	−29	−41

Square Tapers

Since (26) shows that the coupling coefficient at cutoff frequency is zero and mode conversion is very small near cutoff, it seems unnecessary to utilize the same "synthesis" method used earlier to obtain a "sophisticated" profile. In addition, the fabrication of a square taper with "sophisticated" profile is much more difficult. For purposes of experimental comparison with the circular tapers just studied, we design the simplest square taper with a linear slope. In order to reduce reflections with a taper of zero end derivatives, a short parabolic "filet" is fitted at each end, and the square taper (1.79 in to 2.812 in) has the following profile with an arbitrarily chosen length of 15 in:

l from 0 to 1 in $\quad b = 1.79 + 0.03785z^2$

l from 1 to 13 in $\quad b = 1.79 + 0.03785(2z - 1)$

l from 13 to 15 in

$$b = 1.79 + 1.022\left[1 - \frac{1}{54}(z - 15)^2\right]. \tag{30}$$

Note that the "effective length" of the taper is only about 11 in, since the mode conversion at 6425 Mc/s does not start until b becomes larger than 2.0552 in. To complete the required taper we need another transition from 2.812 in square to 2.812 in ID circular. This transition can be made from a mandrel formed by cutting a linear conical taper with $2a_1=2.812$ in and $2a_2=\sqrt{2}\times 2.812$ in, and slicing off four flat sides parallel to the axis such that one end is a circle of 2.812 in ID and the other end is a 2.812 in square. The dominant mode reflections from such a transition of 12 in length are measured to be less than -45 dB. Since the sides of this transition are parallel to the axis, the mode conversion due to this transition should be zero, according to (26) or (10), since $da/dz=db/dz=0$. Because of the gradual flaring at the circular part of corners, this transition may yield comparatively small or negligible TM_{11} mode conversion. The results of measurements are also tabulated in Table I. Comparison shows that the "unsophisticated" "linear" square taper is indeed a strong contender to the "synthesized" circular taper. If the square taper were "synthesized" its mode conversion would be lower than that of the "synthesized" circular taper of the same length.

Conclusions

The coupling coefficient between the TE_{11} mode and the TM_{11} mode in circular waveguide is derived, and at cutoff frequency it tends to approach an infinity of the order of $0^{-1/4}$. The corresponding coupling coefficient between the TE_{10} mode and the TM_{12} mode in rectangular waveguide is also derived, and at cutoff frequency it tends to approach a zero of the order of $0^{1/4}$. Accordingly, for the modes concerned it is theoretically advantageous to design square tapers at and near cutoff frequency in order to reduce mode conversion levels in shorter lengths. On the other hand, the fabrication of a square taper with "sophisticated" profile is much more difficult than the fabrication of a circular taper. Design procedures for a circular taper at and near cutoff are shown, and the experimental results are in agreement with the theoretical calculations. For frequency far away from cutoff, the choice between the circular taper and the rectangular taper is insignificant.

In circular waveguide tapers the coupling of the TM_{11} mode due to the presence of the TE_{11} mode is of the voltage type, whereas in rectangular or square waveguide tapers the coupling of the TM_{12} mode due to the presence of the TE_{10} mode is of the current type. The

difference between the coupling mechanisms in these two cases could be responsible for the drastically different behaviors at the cutoff, but no convincing physical interpretation can yet be offered.

Acknowledgment

The author wishes to thank Mrs. C. M. Kimme for her assistance in carrying out the computational program, and Loren Dale for his assistance in making the measurements.

References

[1] H. Unger, "Circular waveguide taper of improved design," *Bell Sys. Tech. J.*, vol. 37, pp. 899–912, July 1958.
[2] S. K. Savvirykh, "On the theory of tapered circular waveguides," *Radiotekhn. i Elektron.*, vol. 4, pp. 472–1002, April 1959.
[3] C. C. H. Tang, "Optimization of waveguide tapers capable of multimode propagation," *IRE Transactions on Microwave Theory and Techniques*, vol. MTT-9, pp. 442–452, September 1961.
[4] S. A. Schelkunoff, "Conversion of Maxwell's equations into generalized telegraphist's equations," *Bell Sys. Tech. J.*, vol. 34, pp. 995–1043, September 1955.
[5] Y. Klinger, "The measurement of spurious modes in over-moded waveguides," *Proc. IEEE (London)*, vol. 106, Pt. B Suppl., pp. 89–99, January 1959.

Computation of the Performance of the Abrupt Junction Varactor Doubler

ALFRED I. GRAYZEL, MEMBER, IEEE

***Abstract*—A computational procedure is given for the solution of the large signal abrupt junction varactor doubler as the input frequency is varied, given the available power of the source and the source and load impedances. The basic equations are presented in a convenient form. The steps in the procedure are then outlined, and an example is given to demonstrate their use.**

Symbols

E_{ff} = efficiency of doubler
E_g = Thévenin equivalent voltage of input source
m_1 = normalized elastance coefficient at input frequency
m_2 = normalized elastance coefficient at output frequency
$\overline{P}$ = parameter defined by (8)
P_{av} = available power of source
P_{in} = input power to doubler
P_{norm} = normalization power $= (V_B+\phi)^2/R_S$
Q_{min} = charge on varactor when $S(t)=0$
q_ϕ = charge on varactor due to contact potential
R_g = real part of Thévenin equivalent source impedance
$\overline{R}_2$ = real part of $(Z_2+R_S+S_0/2j\omega)/RS$
R_S = series resistance of the varactor
S_0 = average value of $S(t)$
$S(t)$ = instantaneous value of elastance
S_{max} = value of $S(t)$ at breakdown
S_{min} = minimum value of $S(t)$
$u \triangleq (2m_2/m_1)^2$
V_B = breakdown voltage
V_0 = direct voltage across varactor
VSWR = voltage standing wave ratio
X_g = imaginary part of Thévenin equivalent source impedance
$y \triangleq m_2(\omega_c/\omega)\cos\theta$
$Z_{bb'}$ = impedance looking into terminals bb' (Fig. 1)
Z_{in} = voltage across diode at input frequency divided by current at input frequency
Z_2 = load impedance
ω = input frequency
ω_c = cutoff frequency of varactor $= S_{max}/R_S$
θ = phase angle by which input current leads output current
$\rho_{aa'}$ = reflection coefficient at terminals aa' (Fig. 4)
$\rho_{bb'}$ = reflection coefficient at terminals bb' (Fig. 4)
ϕ = contact potential
ψ_A = angle at which $S(t)$ is a maximum
ψ_B = angle at which $S(t)$ is a minimum

Manuscript received October 14, 1965; revised February 14, 1966.
The author is with the Lincoln Laboratory, Massachusetts Institute of Technology, Lexington, Mass. (Operated with support from the U. S. Air Force.)

Introduction

HAVING DESIGNED a doubler circuit quite often, one would like to know its efficiency and output power as the input frequency is varied about the design frequency. In this paper we therefore consider the following problem: Given an abrupt junction varactor doubler circuit whose load and source impedances have already been chosen, driven by a sinusoidal source whose frequency we are free to vary and whose available power is a known function of frequency, what is the output power and efficiency as a function